ACS APPLIED MATERIALS & INTERFACES

Research Article

www.acsami.org

Surface Modification of Cured Cement Pastes by Silane Coupling Agents

Andrew Stewart, Brett Schlosser, and Elliot P. Douglas*

Department of Material Science and Engineering, University of Florida, Box 116400, Gainesville, Florida 32611, United States

Supporting Information

ABSTRACT: X-ray photoelectron spectroscopy (XPS) and static contact angle measurements were used to study the interaction between silane coupling agents and cured cement paste. Three different silane coupling agents were investigated: aminopropyltriethoxy silane (APTES), 3-glycidyloxypropyltrimethoxy silane (GPTMS), and methoxy-terminated polydimethxyl siloxane (PDMS). These silanes have different end groups, so the change in surface energy after undergoing a successful reaction between the silane and hydroxyls on the surface of the cement paste was demonstrated by a change in contact angle. Relative to untreated samples, APTES samples decreased the contact angle, PDMS samples increased the contact angle, and GPTMS did not show a significant change in contact angle. Samples with a water-to-cement ratio (w/c) of 0.5 showed a larger change in contact angle than 0.4 w/c ratio samples, because of a greater number of hydroxyl groups at the surface. Deconvolution of the O 1s and Si 2p XPS peaks were performed to determine contributions from bridging and nonbridging atoms. An increase in bridging silicon and oxygen atoms relative to untreated samples indicated successful silane condensation and that a covalent bond was formed between the cement paste and silanes.

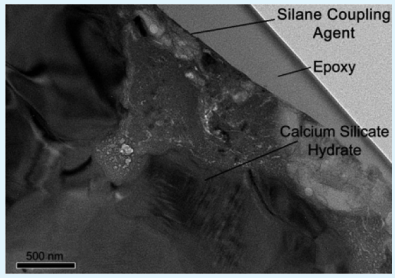

KEYWORDS: *epoxy, concrete, FTIR, NMR, cement paste*

INTRODUCTION

Repair and rehabilitation of civil infrastructure in the United States is of great concern, and approaches that can reduce the cost and time of repairs are needed. One common approach is the use of epoxy/fiber composites to strengthen bridges and other systems that have been damaged or no longer meet the load requirements. These repairs are considered "bond critical", in that the strengthening mechanism relies on good adhesion at the composite/concrete interface. However, there is much evidence showing that the current methods and practices are not adequately resistant to environmental conditions. The mechanism of bond degradation proposed by numerous authors suggests that, when epoxy is exposed to water, the water molecules replace epoxy−concrete hydrogen bonds with water−epoxy hydrogen bonds.[1,2]

One approach recently proposed to improve the environmental durability of the epoxy/cement interface is the application of silane coupling agents. While this approach has been extensively investigated for metal/epoxy systems, it is not well understood when applied to cement. Several studies (reviewed below), including our own previous work, shows that the application of silane coupling agents improves the durability of the system as determined by mechanical measurements. However, the mechanism of this improvement has not been investigated. In the case of metals, the reaction mechanism of a silane coupling agent with the metal oxide layer has been studied in depth by many researchers.[3,4] Silicone is the center of the silane molecule that contains an organic functional group (Y) and alkoxy functional groups (OR). The alkoxy groups become hydroxyl groups (OH) with hydrolysis, and then form an alcohol (R−OH). Over the course of the reaction, hydroxyl groups condense with each other, as a result of dehydration. The end product is a chemical bond between an inorganic (e.g., cement) and organic (e.g., silane coupling agent) material. Since hydrolysis and condensation are dependent on pH and catalysts, typically, a weak acid such as acetic acid is used in the procedure to ensure that the rate of hydrolysis is much greater than the rate of condensation. A comparable understanding of silane functionalization of cement currently is not available, largely because of the complex nature of the cement surface. Calcium-silicate-hydrate (CSH, the primary component of hydrated cement) appears to have silanol groups on the surface, although the surface composition may change and the surface charge can be positive or negative, depending on the presence of ions[5−7] and the water content.[8,9] X-ray photoelectron measurements show that the cement surface may be carbonated (i.e., have a layer of calcium carbonate), because of exposure to the ambient atmosphere.[8] Thus, it is not clear whether silane coupling agents can react with the cement surface. As a result, two possible mechanisms have been proposed for the improvement in durability:[10,11]

(1) The silane coupling agent forms a covalent bond between the cement and the epoxy, preventing water molecules from disrupting the interfacial bonding. This mechanism requires that the silane reacts with the cement surface.

Received: September 12, 2012
Accepted: January 11, 2013
Published: January 11, 2013

(2) The silane coupling agent acts as a hydrophobic barrier, preventing lateral diffusion of water at the interface. This mechanism would not require that the silane react with the cement surface.

Our overall goal in this paper is to examine whether or not a condensation reaction occurs between silane coupling agents and cement. Through direct spectroscopic measurements, we are able to show successful reaction in this system, which is the first time that such a reaction has been shown to occur. The results thus provide new information on the mechanism of durability enhancement in these materials.

BACKGROUND

Little work has been done on direct surface modification of concrete; however, some work has been done on other systems, such as ceramic tiles. Mansur et al. used silane-modified glass tiles that were bonded to modified cement mortars containing poly(ethylene-co-vinyl acetate)[12] or poly(vinyl alcohol)[13] with a water-to-cement (w/c) ratio of 0.6. They found improved interfacial strength, which was attributed to the formation of covalent bonds between the polymer and ceramic.

Another area where silanes have been used on ceramic systems is in the field of dentistry. A recent review of over 100 articles summarized that the preferred bonding method for these silica-based ceramics is hydrofluoric acid (HF) etching and subsequent silane treatments.[14] Numerous articles in the review suggested that mechanical bonding is also important in these systems, which is achieved by grinding, air abrasion, or acid etching. In a different article, by Hooshmand et al., a silane coupling agent was applied to a ceramic surface and evaluated for tensile strength.[15] Different surface preparations before silane application were performed, including polishing, gritblasting, HF etching, and combination of gritblasting and etching. The durability of the ceramic was evaluated by storing the sample in water at various temperatures for up to 3 months. The results indicated a durable tensile bond could be achieved by appropriate silane application without the use of HF etching and that the silane bond was capable of resisting hydrolytic attack in boiling water.

Previous work on this topic by in our research group has demonstrated that the application of an epoxy-functional silane coupling agent can decrease the detrimental effect of water on the concrete−epoxy bond.[11] This was attributed to the formation of covalent bonds, as well as a decrease in the diffusivity of water due to the hydrophobic silane.[10] Slant shear measurements of the interfacial strength indicated that the application of the epoxy functional silane coupling agent led to significant improvement in the durability of concrete cylinders exposed to water from 30 to 60 °C over a 12-week period. However, as with the silane−ceramic work found in the literature, this work did not examine the mechanism by which the improvement in durability was achieved. In this paper, we begin to address that question by investigating chemical modification of the cement surface at a chemical level.

In order to determine how silane coupling agents affect the surface properties of materials, one of the most commonly used techniques is contact angle measurement. The relation between the contact angle and interfacial energy of a liquid and a solid is explained with the Young−Dupre equation:

$$0 = \gamma_{SG} - \gamma_{SL} - \gamma \cos \theta_c \quad (1)$$

where γ_{SG} is the solid−vapor interfacial energy, γ_{SL} the solid−liquid interfacial energy, γ the liquid−vapor interfacial energy, and θ_C the equilibrium contact angle. As can be seen from the above equation, wetting of a solid surface that has a high surface energy, such as a ceramic, can be achieved more readily than wetting a low surface energy surface, such as a polymer. On a smooth and flat surface, contact angle measurements are easy to perform. However, because of the nature of cementitious surfaces, surface roughness, cavities, and pores make these measurements difficult.[16] Wenzel introduced the roughness ratio (r) to quantify this surface roughness effect in the Young−Dupre equation:[17]

$$\cos \theta_A = r \cos \theta \quad (2)$$

where θ_A is the apparent contact angle and r is the ratio of the real rough surface area to the ideal smooth surface. Note that, for rough surfaces, $r > 1$ and, for a perfectly smooth surface, $r = 1$. Although Wenzel's equation shows that there is a difference between rough surfaces and smooth surfaces, it does not describe contact angle hysteresis.

While the roughness factor introduced by Wenzel may describe surfaces with homogeneous roughness, on some surfaces, the roughness may be nonuniform. On rough surfaces, a wetting liquid will not be completely absorbed by the surface cavities, while a nonwetting liquid may not penetrate into pores. This will result in the formation of air pockets. Cassie and Baxter extended the Wenzel equation to account for nonhomogenous surfaces with cavities and pores:[18]

$$\cos \theta_A = r_f f \cos \theta_0 + f - 1 \quad (3)$$

where r_f is the roughness ratio of the wet surface and f is the fraction of solid surface area wet by the liquid.

A different study on a variety of materials, including ceramics, polymers, and metals, have found a direct correlation between surface roughness (from 0.2 μm to 8 μm) and contact angle.[19] Kubiak et al. combined the Wenzel and Cassie−Baxter theories with 2D surface morphology analysis and developed the following equation:

$$\cos \theta_A = \left(1 + \frac{R_{Lo}}{100\%}\right)\left(\frac{R_{mr}}{100\%}\right)[(\cos \theta) + 1] - 1 \quad (4)$$

where θ is the contact angle for the ideal surface, θ_A the measured contact angle, R_{Lo} the length of the roughness profile (expressed in terms of % expansion from the smooth profile), and R_{mr} the relative material ratio of the roughness profile measured in the vertical position. In experimental measurements, they measured a minimum contact angle, which corresponded to a roughness of 0.3−1 μm, measured by optical interferometric profilometry, depending on the material. The most variation was found in ceramic and copper alloy samples with minima in the contact angle at an average roughness of ∼1 μm.

Momber directly examined the contact angle of cement paste and concrete and found a decrease in the contact angle with gritblasting and sawing, but also acknowledged that more investigations are necessary to determine a relationship between contact angle and the location of measurement.[20] Our study avoids these issues by polishing samples to a uniform surface roughness and avoiding measurements on areas with grooves or areas with irregular surfaces.

While much research has been dedicated to the impact of surface roughness on concrete strength, fundamental issues

regarding the interfacial bond have been overlooked.[21,22] For the most part, past research has only investigated the microscale and assumed that the surface effect is due to mechanical interlock, while ignoring issues at the nanoscale. Garbacz et al. directly examined mechanical interlock; however, their treatments to vary the roughness resulted in the smoothest, untreated samples having the highest pull-off strength.[23] This was explained by the appearance of voids at the interface for the rougher surfaces.

In summary, then, it seems clear from mechanical testing that the addition of silane coupling agents reduces the detrimental effects of water on the strength of the interface in various inorganic/organic systems. For cement/epoxy specifically, the mechanism of this improved durability has not been investigated using direct spectroscopic techniques, and the complex nature of the cement surface leads to some uncertainty as to whether or not the improvement is due to the formation of covalent bonds. This study is the first to show that silanes can be condensed onto the surface of cement to form covalent bonds, and that the chemistry at the cement surface can be modified by appropriate choice of the coupling agent.

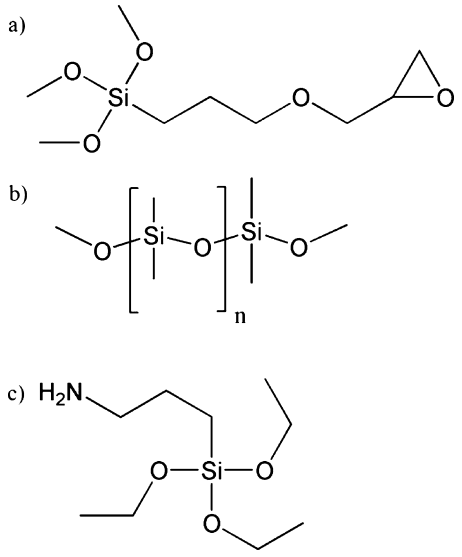

Figure 1. Chemical structure of (a) GPTMS, (b) PDMS, and (c) APTES.

EXPERIMENTAL PROCEDURE

Commercial Florida portland Type I/II cement was used to prepare cement pastes with water to cement (w/c) ratios of 0.4 and 0.5 to evaluate the effect of different chemical compositions on silane treatment. After vigorous hand mixing for 5 min, the pastes were transferred to 4 cm × 4 cm Teflon molds and cured at room temperature for 1 week. After 1 week, samples were demolded and transferred to a limewater solution to cure for 3 weeks to complete the hydration process. Next, the samples were polished by hand, using sandpaper of increasing grit size (from 300 to 1200). In order to further reduce surface roughness and improve uniformity, a Model 120 South Bay Technology lapping and polishing machine was used, first with 300 grit sandpaper, followed by 800 grit sandpaper, until the surface developed a smooth, near-mirror finish. Surface roughness was assumed to be uniform for all samples, because of automated polishing, as demonstrated in the literature.[15,16] After polishing, all samples were cleaned with hexane in a sonicator for ∼5 min and then rinsed with deionized water. Miller et al. have demonstrated the ability of automated polishing to attain a mirror finish on concrete mortar.[24]

Polished cement pastes were prepared with three silane coupling agents with specific functionalities, as shown in Figure 1. Aminopropyl triethoxysilane (APTES), 3-glycidyloxypropyl trimethoxysilane (GPTMS), and methoxy-terminated polydimethyl siloxane (PDMS) were chosen, to evaluate their compatibility with cement pastes. The silanes were supplied by Gelest and were used as received without further purification. Monolayers of silane coupling agents were applied to the surface by suspending the cement over liquid silane at 90 °C for 1 h to evaporate and condense the silane on the cement surface. Two samples for each w/c ratio and silane coupling agent combination were prepared.

Tapping-mode atomic force microscopy (AFM) measurements were performed to evaluate the surface roughness of the cement pastes. Both topological and phase images were recorded with a Dimension 3100 system using a Nanoscope V device. The scan rate was 1 Hz (scan line per second) and scan size was 50 μm × 50 μm, using a probe with a cantilever spring constant of 40 N/m and a resonance frequency of ∼270 kHz. The free amplitude (A_0) of the cantilever tip in air was maintained at ∼20 nm, and the set point (A_{sp}/A_0) was automatically determined by the instrument.

Static contact angle measurements were obtained using an autopipetting goniometer (Ramé-Hart, Inc.), along with a lighting system (Schott-Fostec, Inc.). A 5-μL droplet of deionized water was deposited onto the substrate and allowed to stabilize for 1−3 s before capturing an image. These images were then used to determine the contact angle. Measurements were taken at five different locations for each sample.

Fourier transform infrared spectroscopy (FTIR) samples were analyzed on a Magna-IR E.S.P. System 760 Spectrometer with 128 samples and reference scans at 4 cm^{-1} resolution from 600 $cm^{-1}$to 4000 cm^{-1}. DRIFT samples were prepared in a 1:100 ratio, using KBr powder. Spectra were corrected for residual CO_2 and H_2O in the chamber using calibrated spectra in the OMNIC software package.

Survey and multiplex XPS spectra were recorded with a Perkin−Elmer 5100 system with an Al Kα X-ray source operating at 15 kV and 300 mA. Prior to acquiring XPS spectra, samples were dried in a vacuum oven for 1 day at 100 °C to evaporate residual vapors. The samples were mounted to the holder with double-sided adhesive tape and placed in a vacuum of 10^{-8}−10^{-7} Torr. All samples were run in survey mode from 1200 eV to 0 eV with a pass energy of 89.45 eV and high-resolution multiplexes were taken using a pass energy of 35.75 eV and a step size of 0.05 eV. The take-off angle was 45°, relative to the detector. Binding energy positions were calibrated against the adventitious C 1s peak position located at 285 eV. Spectra were analyzed and deconvoluted with AugerScan software.

RESULTS AND DISCUSSION

AFM Measurements. Previous research on cementitious materials using AFM has indicated a variation in mechanical properties between hydrated and unhydrated cement and highlighted the importance of polishing techniques.[25] Miller et al. outlined a specific polishing procedure that takes into consideration the multiphase composite nature of cement paste.[24] Their technique involves grinding with polishing pads, with the sample mounted on a disk using an adhesive and placing a constant weight on top. A slow lapping speed was used for up to 8 h, to minimize sample disturbance. Roughness measurements verified the effectiveness of their procedure, showing a root-mean-square (RMS) roughness of <100 nm after 2 h of polishing that decreased to <30 nm after 4 h.

Figure 2 shows the two-dimensional (2D) and corresponding three-dimensional (3D) height images of our unpolished cement paste. A 50 μm × 50 μm scan size was chosen, so a relatively large area could be analyzed. If a smaller area was used, it would not be representative of a typical sample, since most samples were ∼3 cm × 3 cm. Based on a 50 μm × 50 μm scan size, the RMS roughness of the unpolished sample was

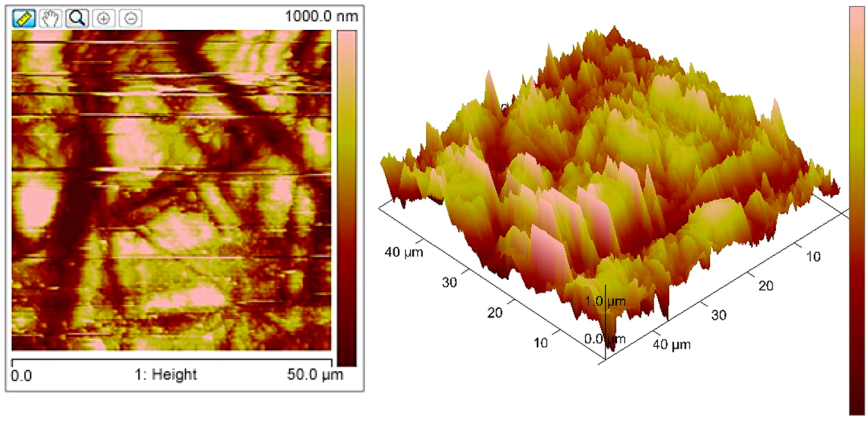

Figure 2. Two-dimensional (2D) and three-dimensional (3D) atomic force microscopy (AFM) height images of unpolished cement paste.

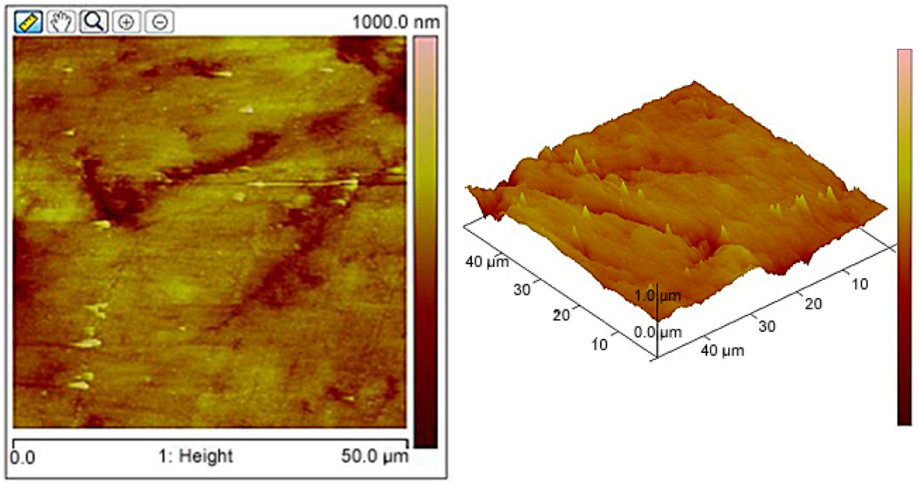

Figure 3. 2D and 3D AFM height images of polished cement paste.

measured to be 318 nm. The horizontal lines represent areas where there was a sudden jump in the AFM tip, corresponding to a dramatic change in height of the cement paste. Using a Detak II A profilometer to measure a 5-mm scan line gave an average roughness of >3 μm.

Figure 3 shows the 2D and 3D height images of polished cement paste. Based on a 50 μm × 50 μm scan size, the RMS roughness was measured to be 84.6 nm. It is clear from the images that the surface is much more uniform, as a result of the polishing technique. Using a Detak II A profilometer to measure a 5-mm scan line gave an average roughness of <1 μm. This roughness lies in the range where small variations will not substantially modify contact angle measurements.[19] Therefore, it can be assumed any roughness introduced by the silane treatment will have a negligible effect on the contact angle measurement.

Contact Angle Measurements. Initial measurements of the contact angle of unpolished cement pastes ranged from 70° to over 100°. This variation correlates well with the results from the aforementioned study on various engineering surfaces by Kubiak et al.[19] In this case, the roughness of the unpolished surface was >3 μm. The cement paste samples polished by hand had a roughness of <1 μm and showed a contact angle of ∼60°. This value is similar to values found in the literature, shown in Table 1; however, the high standard deviation in the data made it necessary to use a more-controlled method, i.e., automated polishing.

Table 1. Measurement of Contact Angles Using Different Techniques on Various Concrete Sample Types

measurement method	source	w/c ratio	sample type	contact angle (deg)
Wilhelmy plate and tensiometer	ref 16	N/A	solution	60
captive drop technique	ref 20	0.60	bulk	50–66
Washburn method	ref 26	0.32	powder	74

Table 2 shows the contact angle measurements before and after treatment of the silane coupling agents. The initial contact angle is represented by the darker color on the left and the final contact angle by the lighter color on the right. For all the samples, the initial contact angle was ∼60°.

Table 2. Contact Angle Measurement of Cement Pastes with w/c Ratios of 0.5 and 0.4 after Silane Treatment

	Initial		After Treatment	
	contact angle (deg)	stdev	contact angle (deg)	stdev
0.5 w/c APTES	61.7	2.4	39.5	4.4
0.4 w/c APTES	57.0	2.2	50.8	2.5
0.5 w/c PDMS	59.4	4.3	76.4	3.2
0.4 w/c PDMS	60.0	1.6	66.3	2.5
0.5 w/c GPTMS	60.8	6.5	61.1	4.0
0.4 w/c GPTMS	62.5	1.5	65.8	4.2

dx.doi.org/10.1021/am301967v | ACS Appl. Mater. Interfaces 2013, 5, 1218–1225

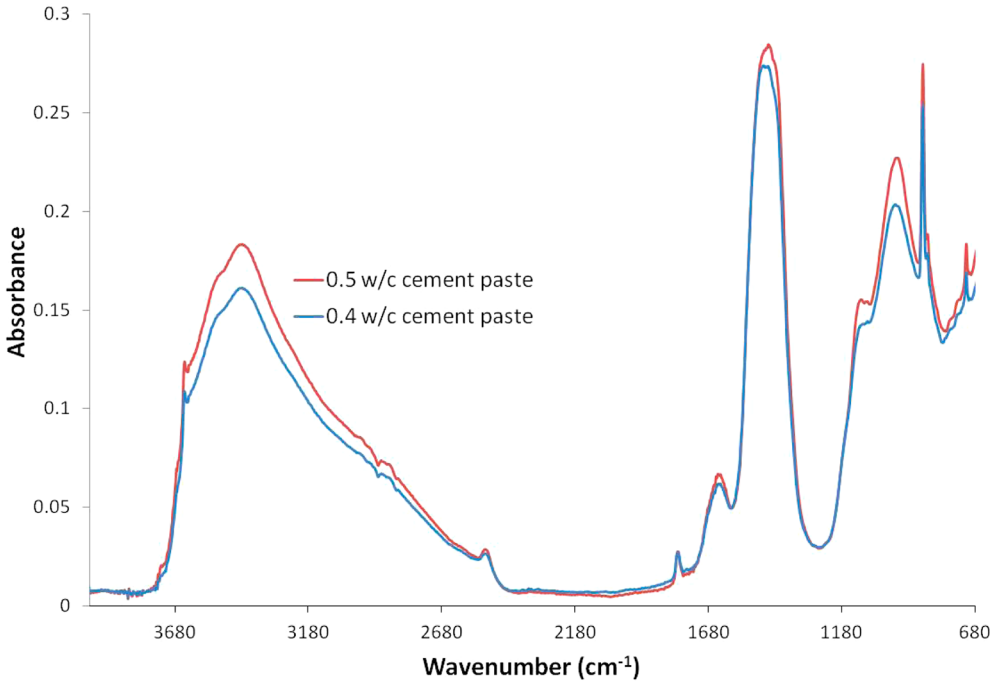

Figure 4. Diffuse reflectance Fourier transform infrared spectroscopy (DRIFT IR) spectra of 0.4 and 0.5 w/c ratio cement pastes.

Overall, APTES decreased the contact angle, while PDMS increased the contact angle. This change in contact angle was expected, since the amino-terminated silane could hydrogen-bond to water during contact angle experiments, while the PDMS silanes would make the surface more hydrophobic. The epoxy-terminated silane (GPTMS) had a negligible effect on the contact angle. The lack of change in the contact angle is most likely due to the epoxy group having neither a hydrophobic or hydrophilic preference. Furthermore, the 0.5 w/c ratio samples demonstrated a greater change in contact angle. As the w/c ratio increases, there is a greater degree of hydration, as a result of curing.[27,28] Therefore, the 0.5 w/c ratio samples are expected to have a greater number of hydroxyl groups or hydrated species, which allows more silanes to interact with the cement paste surface, as compared to 0.4 w/c ratio samples.

Infrared (IR) data confirmed the difference in OH and H_2O present in samples with different w/c ratios (Figure 4). Spectra were linearly baseline-corrected, then normalized to the asymmetric stretching vibration of CO in $CaCO_3$ centered at 1460 cm^{-1}. Visually, it is clear that there is a greater absorbance in OH groups from 3000 cm^{-1} to 3600 cm^{-1} and H_2O at 1650 cm^{-1} for the 0.5 w/c ratio sample, corresponding with a greater degree of hydration. Taking the areas under the OH and H_2O absorbance peaks and dividing by the CO absorbance gave a semiquantitative value for the difference between the two types of cement pastes. Obtaining quantitative values for materials containing silicon has been shown in other studies using diffuse reflectance Fourier transform infrared spectroscopy (DRIFT IR).[29,30] Using this approach, the 0.5 w/c samples had ~28% more hydroxyl groups than the 0.4 w/c samples, but this value is only a rough estimate. The higher number of hydroxyl groups correlates well with the contact angle measurements, which indicated a greater change in contact angle with the greater w/c ratio samples.

While pull-off bond strengths were not performed on the samples, research by Mansur and co-workers on polymer-modified cement-mortar−glass-tile composites indicated an increase in bond strength with a variety of different silanes.[13,31] The suggested mechanism is the formation of a hybrid interface based on hydrogen bonds, where hydroxyl side groups can act as a chemical cross-linking agent between surface silanols and water found in the interlayer space of hydrated cement. In their systems, they used cement mortar modified with poly(ethylene-co-vinyl acetate)[12] or poly(vinyl alcohol)[13] with a w/c ratio of 0.6. The system used in this study uses no sand and a lower w/c ratio; however, their suggested interfacial bonding may be appropriate for comparison. Although Mansur et al. used EVA to promote hydrogen bonding of surface silanols and water in the interlayer space with the polymer, the idea that these two groups are available to come into contact and interact with the silane coupling agent may be a key to the description of the bonding.

A different study by Choi et al. demonstrated improved durability on samples whose surfaces had been treated with an epoxy-functional silane coupling agent.[11] The two proposed mechanisms for that study suggested that the silane interacts with hydrogen-bonding species of concrete to form a covalent linkage after condensation occurs, or the GPTMS directly interacts with the epoxy to prevent moisture uptake.

X-ray Photoelectron Spectroscopy (XPS). To determine the surface chemistry of the silane−cement-paste interaction, XPS experiments were performed. Figure 5 shows XPS survey spectra of the cement paste before and after treatment with the silane coupling agents. The elemental compositions and binding energies are summarized in Table 3.

Although portland cement is composed of other elements besides C, O, Si, and Ca, these elements were chosen because they are the most dominant and easiest to resolve in the XPS spectra. For the samples coated with the silane coupling agents, an increase in the atomic concentration of carbon, along with a decrease in oxygen and calcium, was observed. This trend has been found by other authors investigating cement paste before and after coating.[9,32] In addition, this change in atomic

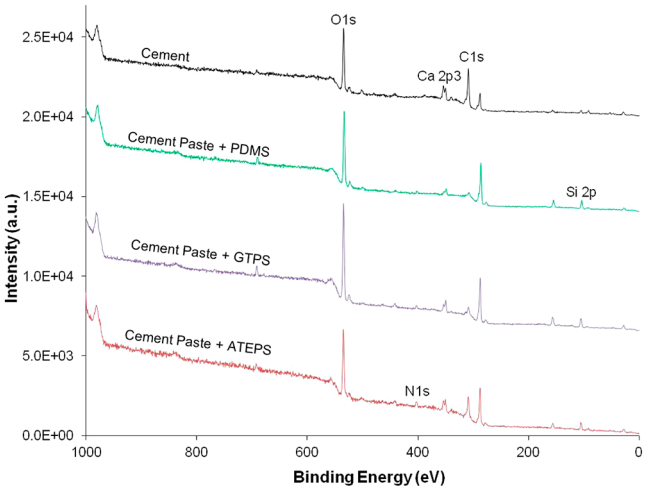

Figure 5. X-ray photoelectron spectroscopy (XPS) survey of treated and untreated cement pastes.

concentration indicates that the silanes were successfully deposited on the cement paste surface, using the evaporation technique. The increase in the silicon composition is due to the silane coupling agent. The small amount of nitrogen found on the silane-deposited samples (<1%), except APTES, is most likely due to oven cross contamination.

In order to examine specific interactions between the silane coupling agent and cement paste, high-resolution XPS data was taken at 0.05 eV intervals. A Shirley background and 80:20 Gaussian/Lorentzian peak shape was assumed in all cases. The C 1s peak for the neat cement paste was fit to two peaks: adventitious carbon at 285 eV and carbonates at 289.5 eV, as also reported by other authors.[32] After silane deposition, the carbonate peak underwent significant attenuation, along with the emergence of a new peak at 285.9−286.7 eV, which is due to the aliphatic carbon chain. No significant changes in the Ca 2p or N 1s binding energies were found. The peak fittings, shown as the dotted lines, for the various electron orbitals are shown in Figures S1−S6 in the Supporting Information. Note that the data have not been corrected for charging effects.

While other authors have shown a change in peak shape and position in XPS spectra after a change in the chemical environment of a material,[33−35] the findings in the current study are more subtle. In order to determine if the silane treatment was successful, O 1s and Si 2p binding energies were fit with two peaks (see data in Table 4). The higher binding energy corresponds to bridging atoms, and the lower binding energy corresponds to nonbridging O atoms. Bridging O atoms are bonded to Si atoms in Si tetrahedral chains, while nonbridging O atoms are typically bound to Ca atoms or hydroxides.[36,37]

Peak fitting of the O 1s line was performed in a method similar to that of Black et al., where an 80:20 Gaussian/Lorentzian peak shape was assumed and a full width at half maximum (fwhm) value of 1.9 eV was used to fit the two types of oxygens.[36] Typical O 1s electron orbitals using these parameters are shown in Figure 6. In this study, the bridging oxygen and nonbridging oxygen contributions of the neat cement paste were determined by fitting the nonbridging oxygen at 531.5 eV and the bridging oxygen at 532.58 eV. The silane-treated samples were also fit to these same values, so comparisons could be made between samples. However, for a few of the samples, an accurate fit using these values could not be made, so the binding energy position was allowed to change up to 0.5 eV. This deconvolution process showed an increase in the number of bridging oxygens, relative to nonbridging oxygens, for all silane treatments. In the condensation step of the silane coupling agent reaction, Si−O bonds are formed between the silane and the substrate and between the silane and itself. If the silanes had not undergone the condensation step, there would be an increase in nonbridging oxygens. Therefore, the increase in bridging oxygens suggests that the various silanes successfully bonded to the cement paste surface.

The Si 2p line was deconvoluted using the same method as the O 1s line, but with a fwhm value of 1.8 eV. Typical Si 2p spectra are shown in Figure 7. Larger fwhm values were tried, but the fittings were of lower accuracy. As with the O 1s fittings, the binding energy positions were kept consistent, so contributions of bridging and nonbridging Si atoms could be determined. Fitting of the Si 2p data showed the same results as for O 1s peaks: an increase in bridging silicons after silane treatment.

SUMMARY

In this study, the effect of various silane treatments on cement paste chemistry was investigated. This investigation examined the hypothesis that hydroxyl groups or hydrated species on cement paste surface may interact with silane coupling agents to create a new functionalized surface. From the atomic force microscopy (AFM) data, care in surface preparation was essential for interpretation of the contact angle changes. Surface roughness has a strong effect on the apparent surface energy in this system. Because of the inherent irregular nature of cement, a uniform surface is essential for acquiring quantitative results. The contact angle data demonstrated successful treatment of the surface with the silane coupling agents. APTES made the surface more hydrophilic, PDMS improved the hydrophobicity of the surface, and GPTES resulted in no significant change. In addition, higher water-to-cement (w/c) ratio samples demonstrated a higher impact on the change in contact angle. Deconvolution of the O 1s and Si 2p electron orbitals were performed to determine contributions from bridging and nonbridging atoms. An increase in bridging Si and O atoms

Table 3. Apparent Surface Composition and Binding Energies of Treated and Untreated Cement Pastes

sample[a]	at. % C	C 1s B.E.[b] (eV)	at. % O	O 1s B.E.[b] (eV)	at. % Ca	Ca 2p B.E.[b] (eV)	at. % Si	Si 2p B.E.[b] (eV)	at. % N	N 1s B.E.[b] (eV)
CP	37.9	285/289.5	46.2	531.7	11.4	347.4/351.1	4.3	102.3	0.2	400.4
CP + PDMS	50.8	285/286.3/289.2	37.0	532.5	2.5	348.0/351.5	8.9	102.7	0.8	400.2
CP + GPTMS	47.3	285/286.2/288.8	38.2	532.3	4.5	347.6/351.2	8.8	102.8	1.1	400.2
CP + ATEPS	49.3	285/286.0/288.9	32.0	532.0	6.6	347.6/351.2	7.6	102.6	4.4	399.7

[a]CP = cement paste; PDMS = methoxy-terminated polydimethyl siloxane; GPTMS = 3-glycidyloxypropyl trimethoxysilane; ATEPS = aminopropyl triethoxysilane. [b]B.E. = binding energy.

Table 4. Binding Energy Positions and Relative Amounts of Bridging and Nonbridging Atoms

	Bridging O 1s		Nonbridging O 1s		Bridging Si 2p		Nonbridging Si 2p	
sample[a]	B.E.[b] (eV)	relative amount (%)	B.E.[b] (eV)	relative amount (%)	B.E.[b] (eV)	relative amount (%)	B.E.[b] (eV)	relative amount (%)
CP	532.58	24.5	531.5	75.5	103.22	21.1	102.16	78.9
CP + PDMS	533.05	53.3	531.9	46.7	103.22	49.4	102.16	50.6
CP + GPTMS	532.77	55.5	531.6	44.5	103.22	57.9	102.16	42.1
CP + APTES	532.58	54.6	531.5	45.4	103.22	41.8	102.16	58.2

[a]CP = cement paste; PDMS = methoxy-terminated polydimethyl siloxane; GPTMS = 3-glycidyloxypropyl trimethoxysilane; ATEPS = aminopropyl triethoxysilane. [b]B.E. = binding energy.

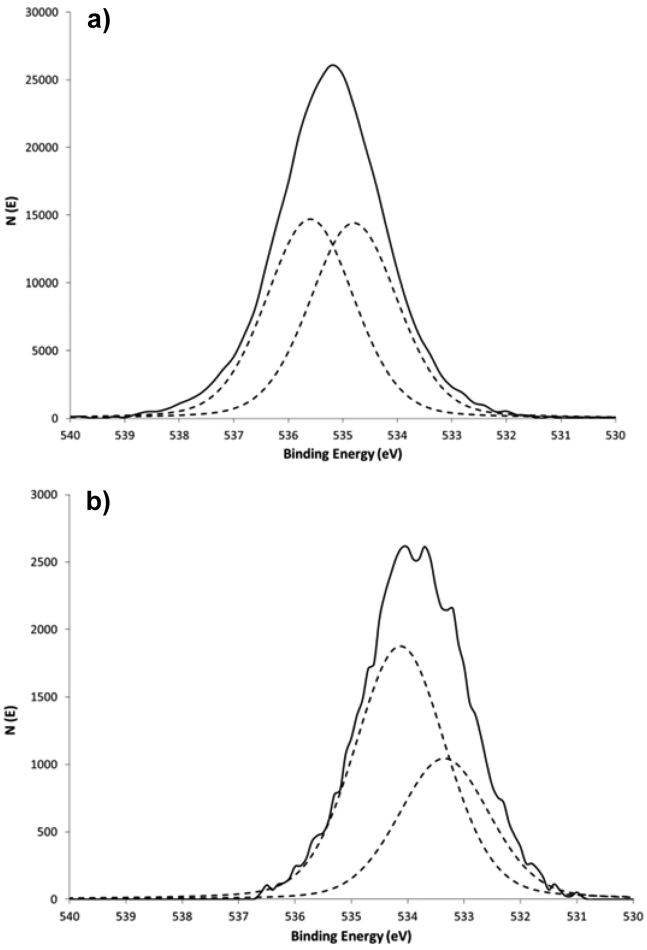

Figure 6. O 1s electron orbital XPS spectra of (a) untreated cement paste and (b) APTES-treated cement paste. Solid line represents the experimental data, dotted lines represent the peak fits.

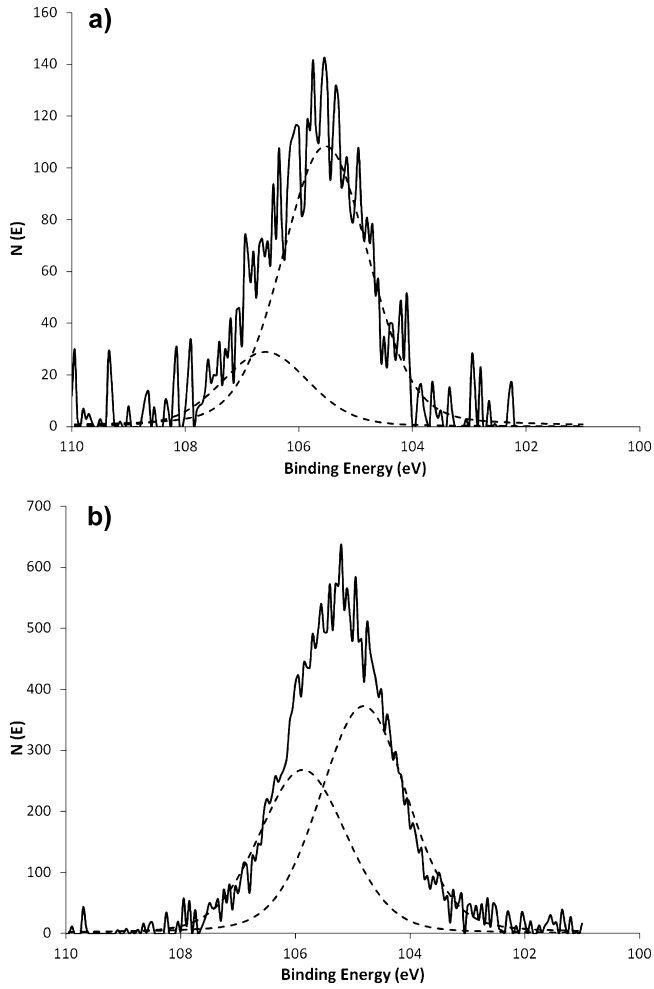

Figure 7. Si 2p electron orbital XPS spectra of (a) untreated cement paste and (b) APTES-treated cement paste. Solid line represents the experimental data, dotted lines represent the peak fits.

indicated successful silane condensation and the formation of a covalent bond between the cement paste and silanes. For all treated samples, the addition of the silane coupling agents caused an increase in bridging Si atoms, because of the covalent linkage. However, the change in contact angle is due to the functional group on the coupling agent.

This study supports previous work by Choi et al.,[11] where cement mortar samples prepared with epoxy and GPTES showed improved durability with water immersion. Changes in the XPS spectra confirmed that the silane reacted with the cement paste, creating a covalent bond, which would not be favorable to water clustering at the cement/epoxy interface. To the best of our knowledge, this is the first study that has addressed the chemical nature of the silane−cement bond, which shows great promise for use in the repair of damaged infrastructure.

■ ASSOCIATED CONTENT

Ⓢ Supporting Information

Supporting Information shows XPS data and peak fittings for untreated cement past and ATEPS treated cement paste. These spectra show the peaks for the C 1s, Ca 2p, and N 1s orbitals. This information is available free of charge via the Internet at http://pubs.acs.org/.

■ AUTHOR INFORMATION

Corresponding Author

*E-mail: edoug@mse.ufl.edu.

Notes

The authors declare no competing financial interest.

■ ACKNOWLEDGMENTS

Funding was provided by the National Cooperative Highway Research Program.

■ REFERENCES

(1) Zhou, J. M.; Lucas, J. P. *Polymer* **1999**, *40*, 5505−5512.
(2) Lefebvre, D. R.; Elliker, P. R.; Takahashi, K. M.; Raju, V. R.; Kaplan, M. L. *J. Adhes. Sci. Technol.* **2000**, *14*, 925−937.
(3) Matinlinna, J. P.; Lassila, L. V. J.; Vallittu, P. K. *Dent. Mater.* **2007**, *23*, 1173−1180.
(4) Meng, X.; Yoshida, K.; Taira, Y.; Kamada, K.; Luo, X. *J. Adhes. Dent.* **2011**, *13*, 71−78.
(5) Merlin, F.; Guitouni, H.; Mouhoubi, H.; Mariot, S.; Vallee, F.; Van Damme, H. *J. Colloid Interface Sci.* **2005**, *281*, 1−10.
(6) Viallis-Terrisse, H.; Nonat, A.; Petit, J. C. *J. Colloid Interface Sci.* **2001**, *244*, 58−65.
(7) Nachbaur, L.; Nkinamubanzi, P. C.; Nonat, A.; Mutin, J. C. *J. Colloid Interface Sci.* **1998**, *202*, 261−268.
(8) Benzarti, K.; Perruchot, C.; Chehimi, M. A. *Colloids Surf., A.* **2006**, *286*, 78−91.
(9) Neves, M. I. B.; Oliva, V.; Mrabet, B.; Connan, C.; Chehimi, M. M.; Delamar, M.; Hutton, S.; Roberts, A.; Benzarti, K. *Surf. Interface Anal.* **2002**, *33*, 834−841.
(10) Ramrus, D. A.; Berg, J. C. *J. Adhes. Sci. Technol.* **2006**, *20*, 1615−1623.
(11) Choi, S.; Maul, S.; Stewart, A.; Hamilton, H. R.; Douglas, E. P. *Polym. Eng. Sci.* **2012**, *53*, 283−294.
(12) Mansur, A. A. P.; Nascimento, O. L. d.; Oréfice, R. L.; Mansur, H. S. *Surf. Interface Anal.* **2011**, *43*, 738−743.
(13) Mansur, A. A. P.; Mansur, H. S. *Cem. Concr. Compos.* **2011**, *33*, 742−748.
(14) Chen, L.; Suh, B. I. *Curr. Res. Dent.* **2012**, *3*, 7−17.
(15) Hooshmand, T.; van Noort, R.; Keshvad, A. *Dent. Mater.* **2002**, *18*, 179−188.
(16) Courard, L.; Michel, F.; Martin, M. *Constr. Build. Mater.* **2011**, *25*, 260−266.
(17) Wenzel, R. N. *Ind. Eng. Chem.* **1936**, *28*, 988−994.
(18) Cassie, A. B. D.; Baxter, S. *Trans. Faraday Soc.* **1944**, *40*, 0546−0550.
(19) Kubiak, K. J.; Wilson, M. C. T.; Mathia, T. G.; Carval, P. *Wear* **2011**, *271*, 523−528.
(20) Momber, A. W. *J. Adhes.* **2002**, *78*, 203−221.
(21) Julio, E.; Branco, F. A. B.; Silva, V. D. *Constr. Build. Mater.* **2004**, *18*, 675−681.
(22) Jones, R.; Chiu, W. K.; Hanna, S. *Theor. Appl. Fract. Mech.* **1994**, *21*, 107−119.
(23) Garbacz, A.; Gorka, M.; Courard, L. *Mag. Concr. Res.* **2005**, *57*, 49−60.
(24) Miller, M.; Bobko, C.; Vandamme, M.; Ulm, F.-J. *Cem. Concr. Res.* **2008**, *38*, 467−476.
(25) Mondal, P.; Shah, S. R.; Marks, L. D. *ACI Mater. J.* **2008**, *105*, 174−179.
(26) Momber, A. W. *Part. Sci. Technol.* **2002**, *20*, 243−246.
(27) Tennis, P. D.; Jennings, H. M. *Cem. Concr. Res.* **2000**, *30*, 855−863.
(28) Bentz, D. P.; Aitcin, P.-C. *Concr. Int.* **2008**, *30*, 51−54.
(29) Klimisch, H. M.; Kohl, G. S.; Sabourin, J. M. *J. Soc. Cosmet. Chem.* **1987**, *38*, 247−262.
(30) Haider, M. M.; Hartinger, I.; Goschl, K.; Demmelmair, A. *Appl. Spectrosc.* **2004**, *58*, 679−682.
(31) Mansur, A. A. P.; Do Nascimento, O. L.; Mansur, H. S. *Surf. Rev. Lett.* **2009**, *16*, 127−139.
(32) Djouani, F.; Connan, C.; Delamar, M.; Chehimi, M. M.; Benzarti, K. *Constr. Build. Mater.* **2011**, *25*, 411−423.
(33) Yousuf, M.; Mollah, A.; Hess, T. R.; Tsai, Y.-N.; Cocke, D. L. *Cem. Concr. Res.* **1993**, *23*, 773−784.
(34) Cocke, D. L.; Mollah, M. Y. A.; Parga, J. R.; Hess, T. R.; Ortego, J. D. *J. Hazard. Mater.* **1992**, *30*, 83−95.
(35) Kallury, K. M. R.; Brennan, J. D.; Krull, U. J. *Anal. Chem.* **1995**, *67*.
(36) Black, L.; Garbev, K.; Stemmermann, P.; Hallam, K. R.; Allen, G. C. *Cem. Concr. Res.* **2003**, *33*, 899−911.
(37) Black, L.; Garbev, K.; Beuchle, G.; Stemmermann, P.; Schild, D. *Cem. Concr. Res.* **2006**, *36*, 1023−1031.